



## **Focusing Properties of Double Ring Shaped Cylindrical Vector Beam by High NA Parabolic Mirror**

**N. Umamageswari<sup>1</sup>, M. Udhayakumar<sup>2</sup>, Haresh M.Pandya<sup>2</sup>, K. B. Rajesh<sup>2\*</sup>**

<sup>1</sup>Department of Physics, Research and Development Centre, Bharathiyar University, Coimbatore, India.

<sup>2</sup>Department of Physics, Chikkanna Government Arts College, Tiruppur, TN, India

Received: 02.06.2014 Accepted: 09.09.2014

### **Abstract**

*The tight focusing properties of double ring shaped cylindrical vector beam focused with a high numerical aperture (NA) parabolic mirror is investigated theoretically by Vector diffraction theory. It shows that the three-dimensional intensity distributions in the vicinity of the focus is dependent on the polarization rotation angle, pupil to beam ratio and numerical aperture value. Additionally, some interesting focal volume structures, such as adjustably confined flat-topped focus, focal spot, and doughnut focal hole can be obtained by controlling polarization rotator angle. The tightly focused double ring shaped cylindrical vector beam by a high numerical aperture parabolic mirror have possible applications in particle acceleration, optical trapping and manipulating, single molecule imaging and high resolution imaging microscopy.*

**Keywords:** Cylindrical vector beam; High NA Mirror; Vector diffraction theory; Optical Trapping.

### **1. INTRODUCTION**

Recently, Intensity distribution in focal region plays an important role in many optical systems, such as in optical tweezers. This makes an increasing interest in laser beams with cylindrical polarization symmetry because the electric field in focal region of such cylindrical vector beam have unique properties (Zhan *et al.* 2009; Youngworth *et al.* 2000), and find wide applications, such as particle guiding or trapping (Gahagan *et al.* 1999; Zhan 2004; Zhan 2003, Veerabagu Suresh *et al.* 2013), scanning optical microscopy (Youngworth and Brown 2000), lithography (Helset *et al.* 2001), laser cutting of metals (Nesterov *et al.* 1999; Niziev *et al.* 1999), particle acceleration (B. Hafizi *et al.* 1997). Among these applications, particular interest has been given to the high numerical aperture (NA) focusing property of these beams and their application as a high-resolution probe. Recently, there is an increasing interest in the higher order (multi-ring) cylindrical vector beams, mostly driven by the advances made in micro-fabrication techniques and theoretical modeling

techniques that were not available with homogeneous polarization (Prabakaran *et al.* 2013; Prabakaran *et al.* 2013; Rajesh *et al.* 2011). The focusing properties of such beam can vary strongly with the filling factor as a result of either destructive interference at the focus between the out-of-phase fields from adjacent rings or from the concentration of intensity at the edge of the aperture as a result of the radial dependence of the field in the associated Laguerre polynomial.

Lens is not the only focusing optical element in a modern microscope. In recent decades, mirrors are of rising interest on high resolution, which is able to enlarge the aperture angle close to  $\pi/2$  (Liu *et al.* 2012; Stadler *et al.* 2008). Since different pupil apodization function fundamentally means different energy transformations between incident wave and outgoing wave, the corresponding vectorial expression are certainly needed to be re-established if a new focusing element is proposed and used particularly for high aperture focusing (Sheppard *et al.* 1997). The apodization factor of a parabolic mirror was originally given by geometrical optics in 1919, and the vectorial

\* K.B.Rajesh Tel.: +919942460031

E-mail: [rajeskb@gmail.com](mailto:rajeskb@gmail.com)

focusing theory for a parabolic mirror based system (PMBS) was discussed in Refs. (Varga *et al.* 2000; Lieb *et al.* 2000; Davidson *et al.* 2004). While high NA parabolic mirrors have been used as efficient light collectors in highly resolved laser spectroscopy of single molecules (Ambrose *et al.* 1991; Fleury *et al.* 1995; van der Meer *et al.* 1995; Durand *et al.* 1999; Enderlein *et al.* 1999), however, for imaging they have been avoided due to their poor off axis imaging performance. Specifically, for the aplanatic lens,  $A(\theta) = \cos^{1/2} \theta$ ; and for the parabolic mirror,  $A(\theta) = 2/(1+\cos\theta)$ . It means that, due to energy conservation, in a parabolic mirror much of the incident energy reaches the focus under high angles while the contrary is valid for an objective lens. Additionally, it can be seen that field components along the mirror axis can arise in the focal region due to the high aperture. Lastly, in parabolic mirror, the component of the electric field which is polarized perpendicular to the plane of incidence causes a phase jump of  $\pi$  when reflection at the mirror surface, which is different from refraction by the aplanatic lens. So the high NA parabolic mirror can be an especially useful alternative for high-NA focusing. In this paper, we wish to analyze the focusing property of the phase modulated double ring shaped CVB tightly focused with high NA parabolic mirror.

## 2. THEORY

At optical frequencies, only the electric field is responsible for the interaction with matter (scattering, fluorescence, excitation, polarization, etc.). Hence only the electric fields will be discussed.

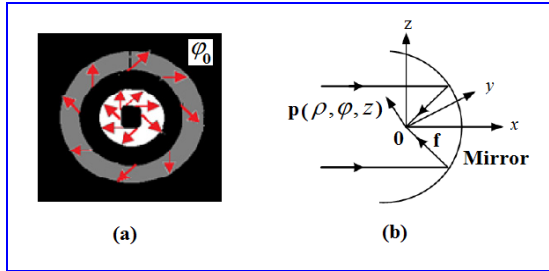


**Fig. 1: (a) Schematic of cylindrical polarized vector beam.  $\phi_0$  is the polarization rotation angle from the radial direction. (b) Diagram of the focusing configuration**

Instead of a radial polarization or an azimuthal polarization, the polarization pattern of each point of the optical beam has a polarization rotated by  $\phi_0$  from its radial direction, as shown in Fig. 1(a). Such a beam is incident upon a high aperture parabolic mirror and then focused on the focus as shown in Fig. 1 (b). The

analysis was performed on the basis of Richards and Wolf's vectorial diffraction method widely used for high-NA mirror system at arbitrary incident polarization (Richards *et al.* 1959). Mathematically, the generalized cylindrical vector beam can be expressed as (Rao *et al.* 2009).

$$E(\rho, \varphi) = l_0(r)(\cos \varphi_0 e_\rho + \sin \varphi_0 e_\varphi) \exp(in\varphi) \rightarrow (1)$$

where  $l_0(r)$  is complex amplitude distribution of the beam,  $\exp(in\varphi)$  is a helical phase term and  $n$  the topological charge. It can be seen in Eq. (1), the relative strength of the radial and azimuthal components is determined by the rotation angle  $\varphi_0$ . By using of Richards–Wolf vectorial diffraction theory, the electric field near the focus at point P can be obtained

$$E^s = -\frac{ikf}{2\pi} \int_{\alpha_0}^{\alpha} \int_0^{2\pi} E_f(\theta, \varphi) e^{ik_s \cdot r_p} \sin \theta d\theta d\varphi \rightarrow (2)$$

Where  $E_f$  is the electric field at the focal sphere, which can be calculated by geometrical optics rules (Lieb *et al.* 2001)

$$E_f = -\frac{2l_0(\theta)}{1+\cos\theta} \cos\theta \cos\varphi e_x + \cos\theta \sin\varphi e_y + \sin\theta e_z \rightarrow (3)$$

where  $2/(1+\cos\theta)$  and  $l_0(\theta)$  are the apodization factor and pupil apodization function for the parabolic mirror, respectively. Considering that the beam being reflected inverted direction of propagation of light in the negative  $z$  direction, the evaluation of the scalar product  $k_s \cdot r_p$  in the exponential term of equation yields negative (Youngworth *et al.* 2000; Richards *et al.* 1959)

$$e^{ik_s \cdot r_p} = \exp[(-ik_s \cos\theta) - ik\rho_s \sin\theta \cos(\varphi - \varphi_s)] \rightarrow (4)$$

where  $k$  is wave number and  $f$  the focal length. Considering that the azimuthal component of the cylindrically polarized beam which is polarized perpendicular to the plane of incidence causes a phase jump of  $\pi$  when reflection at the mirror surface in parabolic mirror focusing, azimuthal electric field changes sign. Substituting Eq. (3) and Eq. (4) into Eq. (2) and transforming cartesian coordinates to cylindrical coordinates, the local radial, azimuthal and longitudinal components of  $E_s$  can be calculated as follows

$$E_p(\rho_s, \varphi_s, z_s) = \frac{ikf}{2\pi} \int_0^{2\pi} \int_0^{\alpha} \frac{2\sin\theta_0(\theta)}{1+\cos\theta} \exp(in\varphi) \exp(-ikz_s \cos\theta) \exp[-ik\rho_s \sin\theta \cos(\varphi-\varphi_s)] \times [-\cos\varphi_0 \cos\theta \cos(\varphi-\varphi_s) + \sin\varphi_0 \sin(\varphi-\varphi_s)] d\theta d\varphi \rightarrow (5)$$

$$E_p(\rho_s, \varphi_s, z_s) = -\frac{ikf}{2\pi} \int_0^{2\pi} \int_0^{\alpha} \frac{2\sin\theta_0(\theta)}{1+\cos\theta} \exp(in\varphi) \exp(-ikz_s \cos\theta) \exp[-ik\rho_s \sin\theta \cos(\varphi-\varphi_s)] \times [-\cos\varphi_0 \cos\theta \sin(\varphi-\varphi_s) - \sin\varphi_0 \cos(\varphi-\varphi_s)] d\theta d\varphi \rightarrow (6)$$

$$E_z(\rho_s, \varphi_s, z_s) = -\frac{ikf}{2\pi} \int_0^{2\pi} \int_0^{\alpha} \frac{2\sin\theta_0(\theta)}{1+\cos\theta} \exp(in\varphi) \exp(-ikz_s \cos\theta) \exp[-ik\rho_s \sin\theta \cos(\varphi-\varphi_s)] \times \cos\varphi_0 \sin\theta d\theta d\varphi \rightarrow (7)$$

Where  $\rho, \varphi$  and  $z$  are the radial, azimuthal and longitudinal coordinates of the observation point P in the focal region, respectively. Using the following formulae:

$$\int_0^{2\pi} \exp(in\varphi) \exp(-ik\rho_s \sin\theta \cos(\varphi-\varphi_s)) d\varphi = 2\pi(-i)^n \exp(in\varphi) J_n(k\rho_s \sin\theta) \rightarrow (8)$$

$$\int_0^{2\pi} \cos(\varphi-\varphi_s) \exp[in\varphi - ik\rho_s \sin\theta \cos(\varphi-\varphi_s)] d\varphi.$$

where  $J_n(\cdot), J_{n+1}(\cdot)$  and  $J_{n+1}(\cdot)$  are the Bessel functions of the first kind with order  $n, n+1$  and  $n-1$ , respectively. In the case of the topological charge  $n \neq 0$ , Eqs. (10)-(12) show the focal properties of cylindrical polarized vortex wave by the high NA parabolic mirror.  $A(\theta)$  describes the amplitude modulation and for illumination by a double ring shaped cylindrical vector beam with its waist in the pupil, this function is given by (Rajesh et al. 2011).

$$A(\theta) = \beta^2 \frac{\sin\theta}{\sin^2\alpha} \exp\left[-\left(\beta \frac{\sin\theta}{\sin\alpha}\right)^2\right] L_p^1\left[2\left(\beta \frac{\sin\theta}{\sin\alpha}\right)^2\right] \rightarrow (13)$$

Where  $L_p^1$  is the generalized Laguerre polynomial and  $\beta$  is the ratio of the pupil radius and the incident beam waist in front of the focusing object lens.

### 3. RESULTS

We perform the integration of Eqs. (10,11,12) numerically for NA=1 and  $\lambda=1$ ,  $\alpha=86.4^\circ$ , and  $\alpha_0=18.9^\circ$  f=1. Here, for simplicity, we assume that the refractive index  $n=1$  and  $A=1$ . For all calculation in the length unit is normalized to  $\lambda$  and the energy density is normalized to unity. Fig (2) shows the structure generated for double ring shaped Radially Polarized beam ( $\varphi_0=0^\circ$ ). It is observed from the fig.2 (a), the generated focal structure is a axially splitted focal spots with focal depth of  $1.2 \lambda$ . From the fig.2 (f), We measure the FWHM of the focal spots is  $(0.6\lambda)$ , when  $\beta=1.2$ . However it is observed that by increasing  $\beta$  to

$$= \pi(-i)^{n+1} \exp(in\varphi) [J_{n+1}(k\rho_s \sin\theta) - J_{n-1}(k\rho_s \sin\theta)] \rightarrow (9)$$

Eqs.(5)-(7) can be transformed as following expressions:

$$E_p(\rho_s, \varphi_s, z_s) = \frac{(-i)^n kf}{2} \exp(in\varphi) \cos\varphi_0 \int_0^{\alpha} \frac{2\sin\theta_0(\theta)}{1+\cos\theta} A(\theta) [J_{n+1}(k\rho_s \sin\theta) - J_{n-1}(k\rho_s \sin\theta)] \exp(-ikz_s \cos\theta) d\theta \rightarrow (10)$$

$$E_p(\rho_s, \varphi_s, z_s) = \frac{(-i)^n kf}{2} \exp(in\varphi) \sin\varphi_0 \int_0^{\alpha} \frac{2\sin\theta_0(\theta)}{1+\cos\theta} A(\theta) [J_{n+1}(k\rho_s \sin\theta) - J_{n-1}(k\rho_s \sin\theta)] \exp(-ikz_s \cos\theta) d\theta \rightarrow (11)$$

$$E_z(\rho_s, \varphi_s, z_s) = (-i)^{n+1} kf \exp(in\varphi) \cos\varphi_0 \int_0^{\alpha} \frac{2\sin^2\theta_0(\theta)}{1+\cos\theta} A(\theta) J_n(k\rho_s \sin\theta) \exp(-ikz_s \cos\theta) d\theta \rightarrow (12)$$

1.5, the splitted focal spots joints together and form a focal spot of FWHM of  $(0.35\lambda)$  and focal depth of  $(1.98\lambda)$  and is shown in fig 2(g & b). We also observed that further increasing of  $\beta$  to 1.8 and 2 reduced the focal depth to  $(1.36\lambda)$  and  $(1.27\lambda)$  respectively and are shown in fig 2(c & d). It is also observed that when  $\beta=2.5$ , the FWHM of the focal spot increased to  $(0.51\lambda)$  with focal depth of  $(1.16\lambda)$  and is shown in fig.2(j & e). Hence we can achieve highly confined longitudinal focal field with very large focal depth which finds application in particle trapping, data storage, biomedical imaging, laser drilling, and machining.

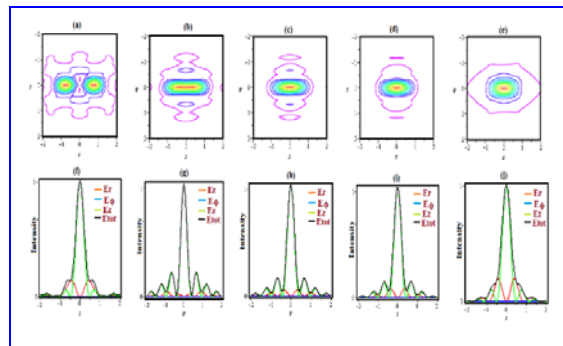


**Fig. 2: Total electric field intensity distributions in the focal region for  $\varphi_0=0^\circ$ , (a)  $\beta=1.2$ , (b)  $1.5$ , (c)  $\beta=1.8$ , d)  $\beta=2$ , e)  $\beta=2.5$  respectively.**

Fig(3) shows the formation of focal structure by double ring shaped azimuthally polarized beam ( $\varphi_0=90^\circ$ ). It is observed from fig.3(a), when  $\beta=1.2$ , the

generated focal segment is a splitted holes each having FWHM of  $(0.7\lambda)$  and focal depth of  $(1\lambda)$  and is shown in fig.3.(f & a).

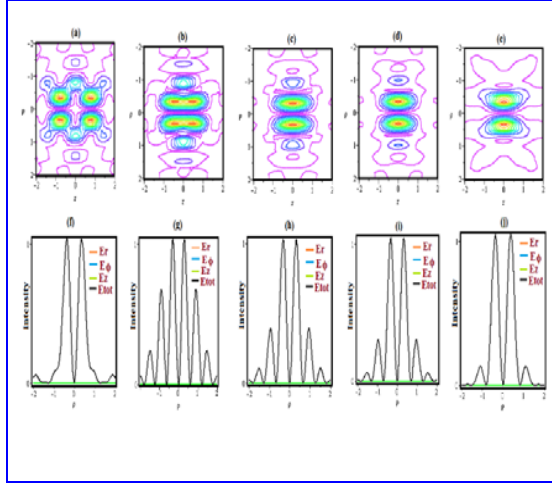


**Fig. 3: Total electric field intensity distributions in the focal region for  $\phi_0 = 90^\circ$ , (a)  $\beta=1.2$ , (b)  $\beta=1.5$ , (c)  $\beta=1.8$  (d)  $\beta=2$  and (e)  $\beta=2.5$  respectively**

Fig.3(b) shows the results for  $\beta=1.5$ , which generates a focal hole of long focal depth of  $(2.2\lambda)$  showing FWHM of  $(0.45)$ . The side hole intensity of the focal hole is found to be  $(0.236\lambda)$  of the main hole. Fig.3(c & d) show further increasing of  $\beta$  to 1.8 and 2 reduced the focal depth to  $(1.6\lambda)$  and  $(1.4\lambda)$  respectively with their corresponding FWHM as  $(0.5\lambda)$  and  $(0.52\lambda)$  and is shown in fig.3.(h & f). It is observed from fig.3(e), further increasing  $\beta$  to 2.5 generates a nonuniform focal hole having much smaller FWHM at the focus as  $(1.18\lambda)$ . It is observed that the size of the focal hole increase in the axial direction. Such a focal hole segment is highly useful for trapping particles with a dielectric constant lower than the ambient.

Fig(4) shows the focal pattern generated for  $(\phi_0=49.6^\circ)$ . It is observed from fig.4(a), the generated focal segment is a two axially splitted focal spots of flat top structure having FWHM of  $(1.92\lambda)$  and focal depth of  $(2.3\lambda)$ . It is observed from fig.4(b), further increasing of  $\beta$  to 1.5 generates a uniform intense flat top structure having focal depth of  $(1.98\lambda)$  and FWHM of  $(0.64\lambda)$ . We observed increasing  $\beta=1.8$  to 2.1 leads to the generation of flat top focal spots with FWHM of  $(0.8\lambda)$  and  $(0.9\lambda)$  and focal depth of  $(1.45\lambda)$  and  $(1.6\lambda)$  respectively.

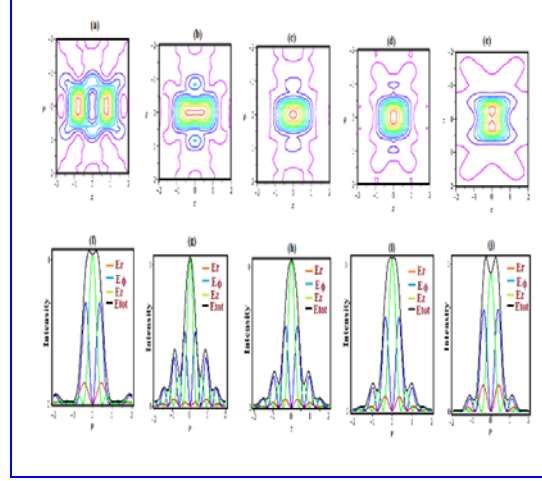


**Fig. 4: Total electric field intensity distributions in the focal region for  $\phi_0 = 49.6^\circ$ , (a)  $\beta=1.2$ , (b)  $\beta=1.5$ , (c)  $\beta=1.8$  (d)  $\beta=2$  and (e)  $\beta=2.5$  respectively**

When  $\beta=2.2$ , the focal depth is further confined to  $(1.12\lambda)$  and FWHM is measured as  $(1.8\lambda)$ . The flat-topped focus obtained above may find some applications such as improved printing filling factor, improved uniformity and quality in materials processing, micro-lithography, and so on. It is observed that by tuning the pupil to beam ratio of  $LG_{(11)}$ \* beam one can tune the focal structure from splitted focal spots/holes to a single focal spot/hole of the long focal depth and can also tune the focal depth. Thus by using double ring shaped beam and by controlling the polarization angle and pupil to beam ratio of the input beam, one can generate many novel focal structures useful for optical micro manipulation near field microscopy.

#### 4. CONCLUSION

The focusing property of high NA parabolic mirror with double ring shaped cylindrically polarized beams is studied. The vector field distributions of cylindrically polarized beams with different pupil to beam ratio by a high NA parabolic mirror are discussed. It shows that various three-dimensional intensity distributions, such as focal spot, focal hole and flat-topped focus, can be obtained by adjusting the polarization rotation angle and the pupil to beam ratio. So the high NA parabolic mirror can be an especially useful alternative for focusing and beam-shaping and single molecule detection.

## REFERENCES

- Ambrose, W. P., Basché, T. and Moerner, W. E., Detection and spectroscopy of single pentacene molecules in a p-terphenyl crystal by means of fluorescence excitation, *J. Chem. Phys.*, 95, 7150-7163 (1991).  
doi:10.1063/1.461392
- Davidson, Nir., Bokor, N. High-numerical-aperture focusing of radially polarized doughnut beams with a parabolic mirror and a flat diffractive lens, *Optics Letters.*, 29, 1318-1320 (2004).  
doi:10.1364/OL.29.001318
- Durand, Y., Woehl, J. C., Viellerobe, B., Göhde, W., and Orrit, M. New design of a cryostat-mounted scanning near-field optical microscope for single molecule spectroscopy, *Rev. Sci. Instrum.* 70, 1318-1325 (1999).  
doi:10.1063/1.1149591
- Enderlein, J., Ruckstuhl, T., and Seeger, S. Highly efficient optical detection of surface-generated fluorescence, *Appl. Optics.*, 38, 724-732 (1999).  
doi:10.1364/AO.38.000724
- Fleury, L., Tamarat, P., Lounis, B., Bernard, J., and Orrit, M. Fluorescence spectra of single pentacene molecules in p-terphenyl at 1.7 K, *Chem. Phys. Lett.*, 236, 87-95 (1995).  
doi:10.1016/0009-2614(95)00185-7
- Veerabagu Suresh, N., Sarasvathi, R. C., Hareesh M.Pandya, Rajesh, K. B., Generation of Multiple Focal Hole Segment by Tight Focusing of Azimuthally Polarised Double Ring Shaped Beam, *J. Environ. Nanotechnol.*, 2, 37-41(2013)  
doi:10.13074/jent.2013.02.nciset36
- Gahagan, K.T., Swartzlander G.A., Jr., Simultaneous trapping of low-index and high-index micro particles observed with an optical-vortex trap, *J. Opt. Soc. Am.*, B, 16, 533-537 (1999).  
doi:10.1364/JOSAB.16.000533
- Helseth, L.E., Roles of polarization, phase and amplitude in solid immersion lens systems, *Opt. Commun.*, 191, 161-172 (2001).  
doi:10.1016/S0030-4018(01)01150-6
- Hafizi, B., Esarey, E., Sprangle, P. Laser-driven acceleration with Bessel beams, *Phys. Rev. E*, 55, 3539-3545 (1997).  
doi:10.1103/PhysRevE.55.3539
- Liu, J., Tan, J., Wilson, T., Zhong, C. Rigorous theory on elliptical mirror focusing for point scanning microscopy, *Optics Express.*, 20, 6175-6184 (2012).  
doi:10.1364/OE.20.006175
- Lieb, M.A., Meixner, A.J. A high numerical aperture parabolic mirror as imaging device for confocal microscopy, *Optics Express.*, 8, 458-474 (2001)  
doi:10.1364/OE.8.000458
- Niziev, V.G., Nesterov, A.V. Influence of beam polarization on laser cutting efficiency, *J. Phys. D: Appl. Phys.*, 32 (13), 1455-1461 (1999).  
doi:10.1088/0022-3727/32/13/304
- Nesterov, A.V., Niziev, V.G. Laser beams with axially symmetric polarization, *J. Phys. D.*, 33, 1817-1822 (1999).  
doi:10.1088/0022-3727/33/15/310
- Prabakaran, K., Rajesh, K.B., Pillai, T.V.S., Chandrasekaran, R., Jaroszewicz, Z. Generation of multiple focal spot and focal hole of sub wavelength scale using phase modulated LG (1,1) beam, *Optik* 124, 5086-5088 (2013).  
doi:10.1016/j.jpleo.2013.03.068
- Prabakaran, K., Rajesh, K.B. and Pillai, T. V. S. Focus shaping of tightly focused TEM<sub>11</sub> mode cylindrically polarized Laguerre Gaussian beam by diffractive optical element, *Optik*, 124, 5039-5041 (2013).  
doi:10.1016/j.jpleo.2013.03.031
- Rajesh, K.B., Veerabagu Suresh, N., Anbarasan, P.M., Gokulakrishnan, K., Mahadevan, G. Tight focusing of double ring shaped radially polarized beam with high NA lens axicon, *J. Optics & Laser Technology.*, 43, 1037-1040 (2011).  
doi:10.1016/j.optlastec.2010.11.009
- Richards B., and Wolf E. Electromagnetic diffraction in optical systems II. Structure of the image field in aplanatic system, *R. Soc. London, Ser. A.*, 253, 358-379(1959).  
doi:10.1098/rspa.1959.0200
- Rao L. Z., Pu J. X. and Chen Z. Y. Focus shaping of cylindrically polarized vortex beams by a high numerical-aperture lens, *Optics & Laser Technology* 41, 241-246 (2009)  
doi:10.1016/j.optlastec.2008.06.012
- Stadler, J., Stanciu, C., Stupperich, C., Meixner, A.J. Tighter focusing with a parabolic mirror, *Optics Letters.*, 33, 681-683 (2008).  
doi:10.1364/OL.33.000681
- Sheppard, C. J. R., Choudhury, A., Gannaway, J. Microwaves, Optics and Acoustics., 1(4), 129 (1977).  
doi:10.1364/JOSAA.17.002090
- Varga, P., Török, P. Focusing of electromagnetic waves by paraboloid mirrors. I. Theory, *Journal of the Optical Society of America A.*, 17, 2081-2089 (2000).  
doi:10.1364/JOSAA.17.002081
- van der Meer, H., Disselhorst, J. A. J. M., Koehler, J., Brouwer, A. C. J., Groenen, E. J. J., and Schmidt, J. An insert for single-molecule magnetic-resonance spectroscopy in an external magnetic field, *Rev. Sci. Instrum.* 66, 4853-4856 (1995)

- [doi:10.1063/1.1146164](https://doi.org/10.1063/1.1146164)  
Youngworth, K.S. and Brown, T. G. Focusing of high numerical aperture cylindrical vector beams, *Opt. Express.*, 7 (2), 77–87 (2000).  
[doi:10.1364/OE.7.000077](https://doi.org/10.1364/OE.7.000077)
- Youngworth, K.S. and Brown, T. G., Inhomogeneous polarization in scanning optical microscopy, *Proc. SPIE*, 3919 (2000).
- Zhan, Q., Trapping metallic Rayleigh particles with radial polarization, *Opt.Express.*, 12 (15), 3377–3382 (2004).  
[doi:10.1364/OPEX.12.003377](https://doi.org/10.1364/OPEX.12.003377)
- Zhan, Q., Radiation forces on a dielectric sphere produced by highly focused cylindrical vector beams, *J. Opt. A: Pure Appl. Opt.*, 5, 229–232 (2003).  
[doi:10.1088/1464-4258/5/3/314](https://doi.org/10.1088/1464-4258/5/3/314)
- Zhan, Q., Cylindrical vector beams: from mathematical concepts to applications, *Adv. Opt. Photon.* 1, 1–57 (2009).  
[doi:10.1364/AOP.1.000001](https://doi.org/10.1364/AOP.1.000001)